Wiley
Advances in Pharmacological and Pharmaceutical Sciences
Volume 2024, Article ID 3048389, 16 pages
https://doi.org/10.1155/adpp/3048389

WILEY

*Research Article*

# Antidiabetic Effect of *Acalypha hispida* Extract and Nanoextract: Mechanism of Action on Pancreatic β-Cell Function via Histone Acetylation

**Hamzah Alfarisi**,[1] **Siti Sa'diah**,[2] **Berry Juliandi**,[3] **and Tutik Wresdiyati**[1]

[1]*Division of Anatomy, Histology, and Embryology, School of Veterinary Medicine and Biomedical Sciences, IPB University, Bogor 16680, Indonesia*
[2]*Division of Pharmacology and Toxicology, School of Veterinary Medicine and Biomedical Sciences, IPB University, Bogor 16680, Indonesia*
[3]*Department of Biology, Faculty of Mathematics and Natural Sciences, IPB University, Bogor 16680, Indonesia*

Correspondence should be addressed to Tutik Wresdiyati; tutikwr@apps.ipb.ac.id

Received 8 May 2024; Revised 14 August 2024; Accepted 11 November 2024

Academic Editor: Kuldeep Singh

Copyright © 2024 Hamzah Alfarisi et al. This is an open access article distributed under the Creative Commons Attribution License, which permits unrestricted use, distribution, and reproduction in any medium, provided the original work is properly cited.

The global prevalence of diabetes mellitus was 537 million in 2021 and is projected to increase to 783 million by 2045. Diabetes progression is also associated with histone modifications. Previous studies have reported that *Acalypha hispida* leaves are rich in flavonoids and phenolic acids, which are associated with antihyperglycemic activity. Recently, we produced a nanoextract of *A. hispida* leaf that contains bioactive compounds with antidiabetic effects. However, there were no studies reported the antidiabetic efficacy of *A. hispida* extract and nanoextract. Hence, we aimed to evaluate the antidiabetic effects of *A. hispida* extract and nanoextract on pancreatic β-cells, insulin secretion, glycogen content, and histone modifications in streptozotocin-induced diabetic rats. Diabetic rats received oral doses of the extract (300 mg/kg bw) and nanoextract (30 and 60 mg/kg bw) daily for 28 days. Bodyweight, blood glucose levels, insulin levels, islets of Langerhans and pancreatic β-cells, glycogen content, acetylation of lysine 9 on histone 3 (H3K9Ac) level, hematology, and lipid profile were assessed. Analyses of variance, principal component analysis (PCA), and partial least squares were performed. The nanoextract of *A. hispida* was successfully produced at a nanosize of 733 nm. The extract (300 mg/kg bw) and nanoextract (60 mg/kg bw) exhibited antidiabetic effects based on the following parameters: decreased blood glucose levels, increased pancreatic β-cell number and density, increased insulin levels, decreased H3K9Ac level in the islets of Langerhans and liver, enhanced glycogen levels in the liver, and improved lipid metabolism. Moreover, PCA indicated that the nanoextract (60 mg/kg bw) showed the strongest antidiabetic effect based on these parameters. The increased β-cell number and density led to decreased blood glucose levels. In conclusion, *A. hispida* extract and nanoextract have antidiabetic effects by restoring β-cell number and density and decreasing H3K9 acetylation in the islets of Langerhans in streptozotocin-induced diabetic rats.

**Keywords:** β-cell; glycogen content; H3K9Ac acetylation; insulin; nanoextract

## 1. Introduction

The International Diabetes Federation approximated that there were 537 million adults diagnosed with diabetes in 2021, which is anticipated to rise to 783 million by 2045 [1]. Diabetes mellitus is defined by heightened blood glucose levels (hyperglycemia), which results in metabolic disorders involving carbohydrates, lipids, and proteins [2]. Hyperglycemic conditions arise from the body's inability to effectively take up glucose into cells, which can be due to insulin resistance, a lack of insulin, or both. Type 1 diabetes is caused by a lack of insulin, while type 2 diabetes is primarily due to insulin resistance [2]. Diabetes treatment aims to maintain blood glucose levels within a target range to

prevent the chronic progression of complications [3]. Multiple categories of medications are employed for the treatment of diabetes, including those that improve insulin sensitivity, stimulate insulin secretion, increase insulin production, slow gastric emptying, and prevent glucose absorption in the kidney [4, 5]. Diabetes drugs have limitations and side effects such as weight gain, anemia, pancreatitis, bladder cancer, hypoglycemia, and digestive problems [6].

Diabetes development and progression are associated with epigenetics, including histone modifications [7]. Histone modifications commonly occur through acetylation and methylation of terminal amino acids in histones 3 and 4 [8]. Acetylation of lysine 9 on histone 3 (H3K9Ac) may also contribute to diabetes progression [9]. H3K9Ac levels are increased in the pancreas of diabetic mice. However, those in the pancreas of diabetic mice are decreased after the administration of exendin-4 treatment [10]. Therefore, the role of H3K9Ac in diabetes remains an active area of research and further research studies are required to achieve a comprehensive understanding of the fundamental mechanisms.

Herbs are used for diabetes treatment as they exert few side effects and are natural, traditional, holistic, cost-effective, and accessible [11]. *Acalypha hispida* is commonly used as an ornamental plant in tropical gardens and can also be grown as a potted indoor plant [12]. Traditionally, the leaves of *A. hispida* have been utilized as diuretics, laxatives, and medicinal properties in treating conditions such as leprosy, abscesses, and kidney disorders [13, 14]. The leaves of *A. hispida* contain polyphenols with hypoglycemic activity, including apigenin, tangeretin, rhoifolin, and phloretin, which have been found to inhibit both $\alpha$-amylase and $\alpha$-glucosidase in vitro and in vivo [15]. In addition, phloridzin and phloretin in leaves have the potential to inhibit glucose transporter 2 (GLUT2) and sodium-glucose transporter 1 (SGLT1), thereby resulting in hypoglycemic effects [15].

*Acalypha hispida* leaf extract is nontoxic, with a lethal dose required to cause death in 50% of the subjects with body weight > 15 g/kg [16] and has a hypoglycemic effect at 300 mg/kg body weight. However, this dose was too high to be converted to a human dose. Therefore, reducing the dose is necessary for patient acceptance. A finer extract size enhances the bioavailability and bioactivity [17]. Utilizing nanotechnology in phytomedicine is an optimal approach for enhancing bioavailability and efficacy [18]. Nanoparticles play a significant role in biomedicine by influencing their stability, drug release profile, mucoadhesion, biodistribution, and cellular uptake (internalization) [19].

Milling methods were used successfully to prepare nanoextracts of *A. hispida* leaves at a nanosize of 520 nm [20] to enable dose reduction for human use. However, no studies have reported the antidiabetic efficacy of *A. hispida* nanoextract. Thus, we aimed to evaluate the antidiabetic effect of the extract and nanoextract of *A. hispida* leaves by analyzing blood glucose levels, insulin levels, islets of Langerhans and pancreatic β-cells, glycogen content, and lipid profile and their mechanism of action via H3K9Ac in diabetic rats.

## 2. Materials and Methods

*2.1. Materials.* *A. hispida* leaves were harvested from Trop-BRC, IPB University, Bogor, Indonesia. The materials used were *A. hispida* leaf, glucometer strips (Accu-Chek, Roche GmbH Germany), STZ (S0130-1, Sigma-Aldrich, St. Louis, Missouri USA), insulin primary antibody (GTX28304, Genetex, Irvine, California USA), acetylated-H3K9AC (A7255, ABclonal, Woburn, Massachusetts USA), Starr Trek Universal Link (STU700H, Biocare, Pacheco, California USA), rat insulin ELISA (E-EL-R3034, Elabscience, Houston, Texas USA), Schiff's reagent (193-08445, Wako), xylene (1.08297.2500, Merck, Darmstadt, Germany), hematoxylin (1.15938.0025, Merck, Darmstadt, Germany), eosin (1.15935.0025, Merck, Darmstadt, Germany), 4% paraformaldehyde (T353-500, Fisher Scientific Company), and ethanol (1.00983.2500, Merck, Darmstadt, Germany).

*2.2. Extraction and Nanoextract Preparation.* *A. hispida* leaves were collected during the dry season, totaling 2 kg. The extraction methods have been reported in a previous study [15]. A total of 1 kg of leaf powder was soaked in 10 L of 96% ethanol for 72 h and filtered. The solvent was evaporated using a spray dryer (inlet 150°C; outlet 90°C). To produce the nanoextract, the dry extract was ground using a FRITSCH planetary ball mill (Pulverisette 7, Germany). The average sizes of the extracts and nanoextracts were measured using a particle size analyzer. These methods have been previously published [20].

*2.3. Quantitative Analysis of Rutin and Quercetin.* The rutin and quercetin contain were measured using HPLC based on the previous method [20]. HPLC analysis was carried out using a Dionex UltiMate 3000 system (Thermo Scientific, USA), which featured a quaternary rapid separation pump (LPG-3400RS) and rapid separation diode array detector (DAD-3000RS). Chromatographic separation was accomplished using a HITACHI LaChrom C18 column, preserved at a persistent temperature of 40°C. Chromatographic analysis was carried out using Chromeleon (c) Dionex Version 7.2.4.8179.

*2.4. Animal Experiment.* Adult male rats (Sprague–Dawley: 250 ± 20 g; 8–12 weeks) were purchased from the National Agency of Drug and Food Control (BPOM), Republic of Indonesia. The rats were acclimatized for 14 days. The cage was controlled at 60%–70% humidity, 25 ± 2°C, and 12:12 light–dark cycles. The sample size was established using the formula by Federer ($t\,(n-1) > 15$) [21], where $t$ represents the treatments and $n$ represents the replications. In total, 30 rats were grouped into six groups ($n = 5$) as follows: a group of normal rats (NL) treated with a vehicle (normal control), diabetic rats (DM) treated with a vehicle (negative control), DM rats treated with metformin at a dose of 88 mg/kg body weight (MF) (positive control), DM rats treated with *A. hispida* extract at a dose of 300 mg/kg body weight (AH),

DM rats treated with *A. hispida* nanoextract at a dose of 30 mg/kg body weight (NA3), and DM rats treated with *A. hispida* nanoextract at a dose of 60 mg/kg body weight (NA6). The extract and nanoextract were dissolved in 1% carboxymethyl cellulose as a vehicle. The extract and nanoextract were administered orally once a day for 28 days.

Diabetic rats received a single intraperitoneal injection of streptozotocin (STZ) at a dose of 55 mg/kg body weight [21]. Three days after induction, blood glucose levels were assessed in diabetic rats, with a blood glucose range of 300–450 mg/dL. The diabetic rats were randomized based on their blood glucose levels, and no significant variations were observed among the groups. Curative treatment was performed for 28 days. Body weight and blood glucose levels were assessed at consistent intervals, including days 0, 4, 8, 12, 16, 20, 24, and 28. Water and feed intakes were recorded daily for the 28-day treatment period. The experimental design was approved by The Animal Ethics Committee School of Veterinary Medicine and Biomedical Sciences IPB University (approval number: 143/KEH/SKE/VI/2019).

*2.5. Sample Preparation.* The rats were anesthetized intraperitoneally with a mixture of ketamine (70 mg/kg body weight) and xylazine (10 mg/kg body weight) on the 29th day. Blood was collected via intracardiac puncture to measure insulin levels and hematological and lipid profiles [22]. Rats were euthanized and then the pancreas and liver were isolated and preserved in 4% paraformaldehyde tissue fixation solution for 8 days [23].

*2.6. Measurement of Serum Insulin.* Blood samples collected in vacutainers were centrifuged at 2000 × g for 10 min to separate the serum. The supernatant was placed in an Eppendorf tube. Insulin levels were assessed using a rat insulin ELISA kit (EEL-R3034, Elabscience, USA) following the manufacturer's instructions [24].

*2.7. Measurement of the Hematological Profile.* The hematological profile included the hemoglobin (Hb) level, hematocrit (Hct) level, erythrocyte count, mean corpuscular volume (MCV), mean corpuscular hemoglobin (MCH), mean corpuscular hemoglobin concentration (MCHC), leukocyte count, and thrombocyte count. Measurements were performed using 5-Diff Hematology Analyzer BC-5000 (Mindray).

*2.8. Measurement of the Lipid Profile.* The measured lipid profiles included triglycerides (TG), total cholesterol (TC), high-density lipoprotein (HDL), very-low-density lipoprotein (VLDL), and atherogenic index (AI). The analysis was performed using a SELECTRA JUNIOR Analyzer (Vital Scientific). VLDL and AI were calculated using the following formulas: (VLDL = TG/5) and (AI: (TG-HDL)/HDL) [25].

*2.9. Hematoxylin-Eosin and Histochemistry Staining.* The pancreas and liver were processed for routine histological assessment, including dehydration, paraffin embedding, sectioning, and staining [23]. The pancreas was stained with hematoxylin and eosin. The liver was stained using periodic acid-Schiff (PAS) to evaluate the glycogen content. The staining methods have been described previously [23]. The magenta color of the PAS stain indicates positive glycogen content. The intensity of the magenta color was measured using ImageJ 1.53q FIJI [26].

*2.10. Immunohistochemistry Staining and Analysis.* The pancreas and liver were subjected to standard histological processing for routine histology assessment [23]. The tissue was sectioned at 5 $\mu$m using a rotary microtome (Sakura), deparaffinized, and rehydrated. The tissue sections were subjected to heat-induced epitope retrieval in citrate buffer at pH 6.0 following a previously reported method [27], with slight modifications. The modification was that the epitope retrieval process was conducted by boiling in a pot until it reached 90°C for 3 min. Then, the pot was transferred to an icebox to cool down to 50°C. Subsequently, the pot was boiled again for 3 min and transferred back to the icebox until it reached 37°C. The tissue was then incubated in normal serum for 90 min and in background sniper for 15 min was used to block nonspecific proteins at 37°C [28]. Anti-insulin primary antibody (GTX28304, Genetex) was incubated overnight to evaluate pancreatic $\beta$-cells. For histone H3 analysis, tissues were incubated with H3K9Ac (A7255, ABclonal). The tissues were then incubated in Trekkie Universal Link and Trek Avidin HRP. The DAB chromogen was used for visualization. The tissues were imaged using a microscope (CX23, Olympus) connected to an Indomicro Digital Camera. The number of pancreatic $\beta$-cells, area of the islets of Langerhans, and intensity of the DAB signal of H3K9Ac were measured using ImageJ 1.53q FIJI [26].

*2.11. Data Analysis.* Data analysis was conducted using one-way ANOVA at a 5% significance level. If a significant effect was observed, Duncan's multiple range test was performed. The Mann–Whitney *U* test was employed when the data did not meet the eligibility criteria for ANOVA, specifically when the data exhibited non-normality or lack of homogeneity. Data analysis was conducted using SPSS 22.00. Data were visualized using GraphPad Prism 9. Principal component analysis (PCA) was conducted to evaluate treatment grouping based on all parameters observed. Partial least squares (PLS) analysis was performed to evaluate the parameters that most strongly affected the blood glucose levels. Multivariate analysis was conducted using SIMCA 14.

## 3. Results and Discussion

The extract and nanoextract of *Acalypha hispida* had the same organoleptic parameters: powder, specific smell, dark green color, and bitter taste (Table 1). Phytochemical analysis showed no difference in the flavonoid, tannin, saponin, and steroid

Table 1: Physicochemical parameters of the extract and nanoextract of *Acalypha hispida*.

| Parameter | Extract | Nanoextract |
|---|---|---|
| Organoleptic | | |
| Form | Powder | Powder |
| Smell | Specific | Specific |
| Color | Dark green | Dark green |
| Taste | Bitter | Bitter |
| Phytochemicals alkaloids | | |
| Wagner | Negative | Negative |
| Mayer | Negative | Negative |
| Dragendorff | Negative | Negative |
| Flavonoids | Positive | Positive |
| Tannins | Positive | Positive |
| Saponins | Positive | Positive |
| Quinones | Negative | Negative |
| Steroids | Positive | Positive |
| Triterpenoids | Negative | Negative |

Table 2: The mean size distribution and polydispersity index of *Acalypha hispida*.

| Sample | Mean size distribution (d·nm) | Polydispersity index |
|---|---|---|
| Extract | 1519.0 ± 107.3 | 0.788 ± 0.030 |
| Nanoextract | 733.1 ± 102.5 | 0.701 ± 0.212 |

Table 3: Presence of rutin and quercetin in *Acalypha hispida*.

| Sample | Rutin (mg/g dry extract) | Quercetin (mg/g dry extract) |
|---|---|---|
| Extract | 0.10 | 0.09 |
| Nanoextract | 0.34 | 0.32 |

contents. The average particle sizes of the extracts and nanoextracts were 1519 and 733 nm, respectively (Table 2). The extract contained 0.10 mg/g of rutin and 0.09 mg/g of quercetin on dry weight (Table 3). The nanoextract contained 0.34 mg/g of rutin and 0.32 mg/g of quercetin on dry weight (Table 3). Based on these data, a nanoextract was successfully produced at a size of 733 nm. The milling process resulted in changes in rutin (5%) and quercetin (10.3%). Milling decreases the average size distribution of bioactive compounds (gallic acid and catechin) [20]. Previous studies have successfully produced nanopowders from *Tridax procumbens* leaves through a milling process, resulting in particle sizes between 114 and 45 nm across varying time periods [29]. This study demonstrated that the duration of milling is crucial for producing homogeneous nanoparticles that enhance the antimicrobial efficacy of *T. procumbens* leaf nanoparticles [29].

Diabetic rats were treated with the extract and nanoextract for 28 days. Figure 1(a) displays the profile of blood glucose levels. After 28 days, the blood glucose profiles of the MF, AH, NA3, and NA6 groups exhibited significantly lower levels compared with those of the DM group (Figure 1(b)) as the AUC values of these groups were significantly lower than those of the DM group ($p < 0.001$). The findings revealed that the extract and nanoextract significantly lowered blood glucose levels.

The MF, AH, NA3, and NA6 groups exhibited significantly lower body weights compared with the NL group on days 20, 24, and 28 ($p < 0.05$; Figures 1(c) and 1(d)). The body weight was significantly higher in the MF and NA6 groups compared with the DM group ($p < 0.05$). These results indicate that the nanoextract at 60 mg/kg body weight showed a significant increase in body weight. Metformin lowers blood glucose levels and increases body weight by activating adenosine monophosphate–activated protein kinase, which helps cells take up glucose [30].

STZ-induced diabetic rats (DM group) showed a significant increase in water and feed intake compared with normal rats (NL group) ($p < 0.001$; Figures 2(a), 2(b), 2(c), 2(d)). However, diabetic rats treated with the extract and nanoextract did not show significant differences in water and feed intake from untreated diabetic rats. These results indicated that diabetes induction using STZ at 55 mg/kg body weight led to symptoms of polydipsia (excessive thirst) and polyphagia (excess consumption) (Figure 2). The STZ dose-induced diabetic rats did not self-recover to a normoglycemic state despite stable diabetic conditions. Previous research has shown that rats induced with a dose of ≥ 50 mg/kg BW of STZ remained consistently hyperglycemic [31].

Figure 3 shows the HE and insulin staining of diabetic pancreatic rats and the observed parameters (Figure 3). The number and density of pancreatic β-cells were diminished in the DM group compared with the NL group ($p < 0.001$; Figures 3(e) and 3(f)). The MF and NA6 groups exhibited a higher quantity of pancreatic β-cells than that of the DM group (Figure 3(e)) and the MF, AH, and NA6 groups showed a higher density of pancreatic β-cells compared with the DM group (Figure 3(f)). The decrease in the number and density of pancreatic β cells was not followed by a significant reduction in the number of islets of Langerhans between treatment groups (Figure 3(c)). These results demonstrated that the extract and nanoextract (60 mg/kg body weight) maintained the number and density of pancreatic β-cells.

The NL group demonstrated a significantly higher insulin levels compared to the DM group ($p = 0.024$; Figure 3(g)). The NA6 group showed the highest insulin secretion. These results revealed that diabetic rats treated with 60 mg/kg body weight nanoextract showed increased insulin secretion and were supported by the similarity in the number and density of β-pancreatic cells between the NA6 and MF groups (Figures 3(b) and 3(c)). However, the NA6 group showed higher insulin levels than that of the MF group (Figure 3(g)).

Extract and nanoextract (60 mg/kg body weight) inhibited the death of pancreatic $\beta$-cell in diabetic rats (Figures 3(e) and 3(f)). This ability was related to its antioxidant content (rutin and quercetin), which can reduce the concentration of reactive oxygen species in pancreatic $\beta$-cells induced by STZ [32]. In our previous study, we observed an increase in Cu/Zn-superoxide dismutase levels in the islets of Langerhans of diabetic rats treated with *A. hispida* and its nanoextracts [33]. In addition, increasing Cu/Zn-superoxide dismutase levels in the pancreas can maintain the number of pancreatic $\beta$-cells in rats administered STZ or alloxan [28, 33].

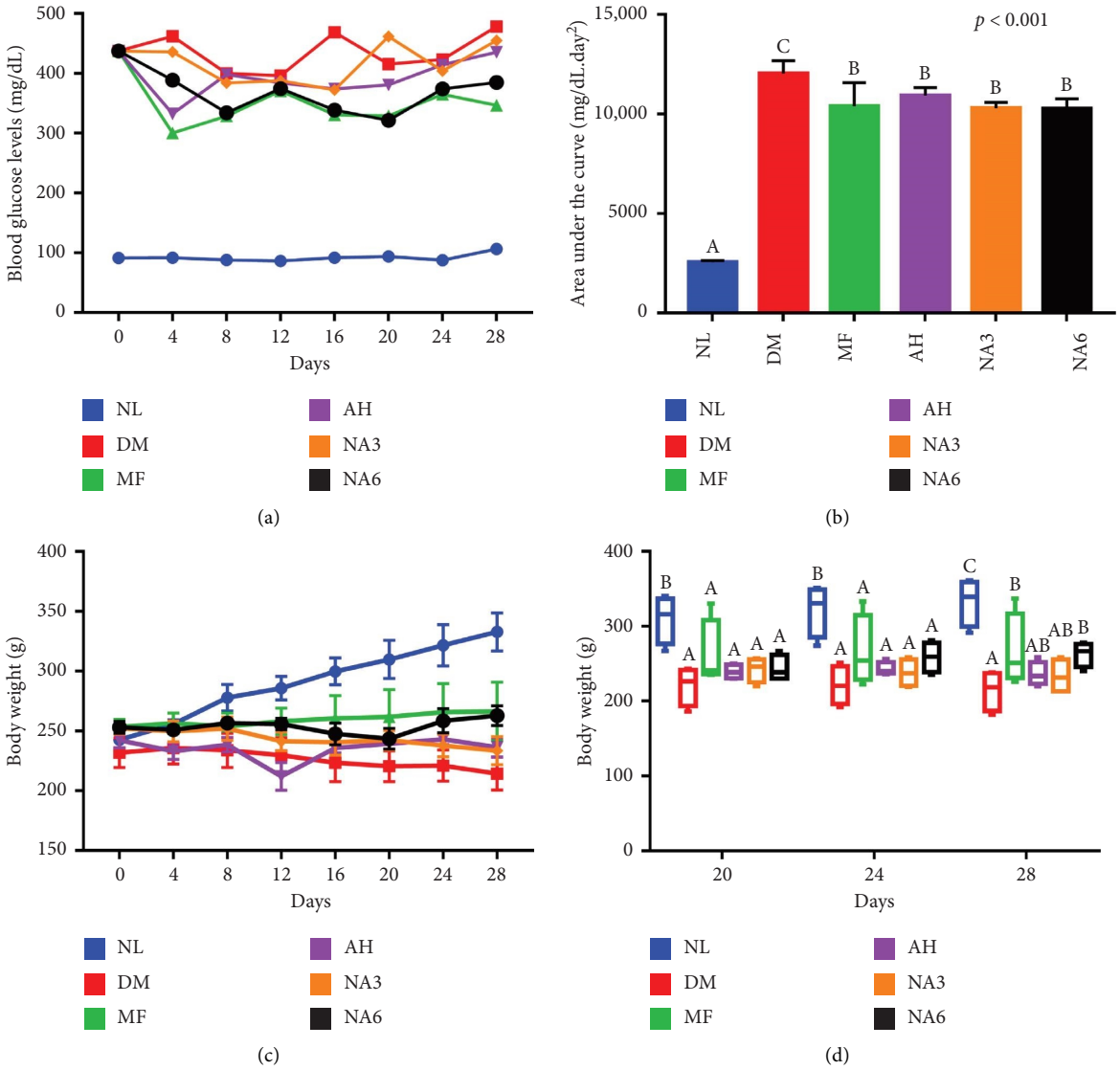



Figure 1: Effect of *Acalypha hispida* extract and nanoextract on blood glucose levels and body weight of diabetic rats. (a) The profile of blood glucose levels for 28 days, (b) area under the curve of blood glucose levels, (c) the profile of bodyweight for 28 days, and (d) bodyweight on 20th, 24th, and 28th. Values are shown as mean ± SD ($n = 4$). Identical letters (A–C) mean no significant differences in DMRT ($\alpha = 0.05$).

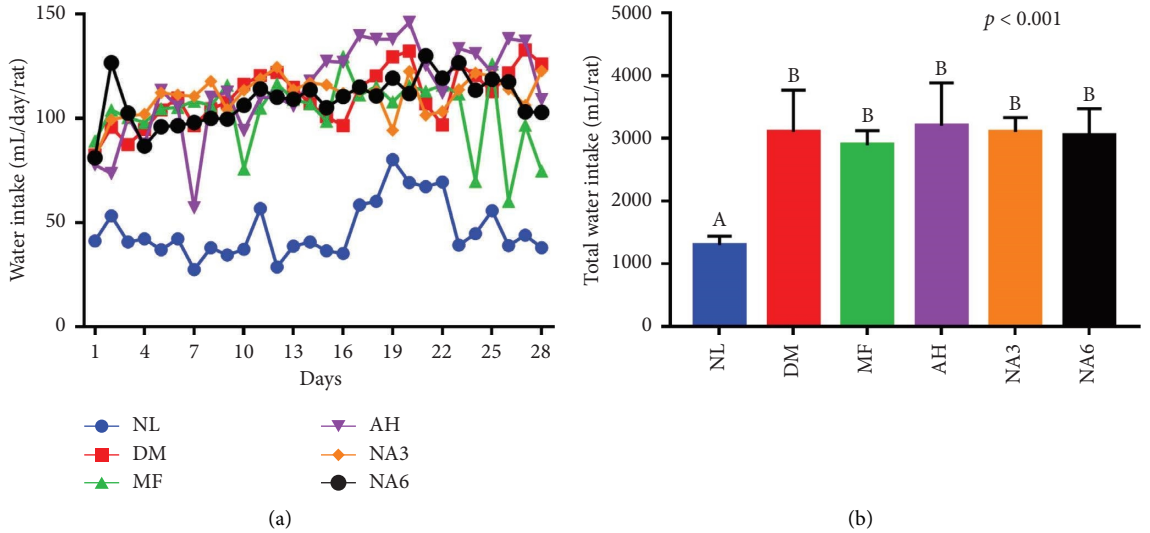



Figure 2: Continued.

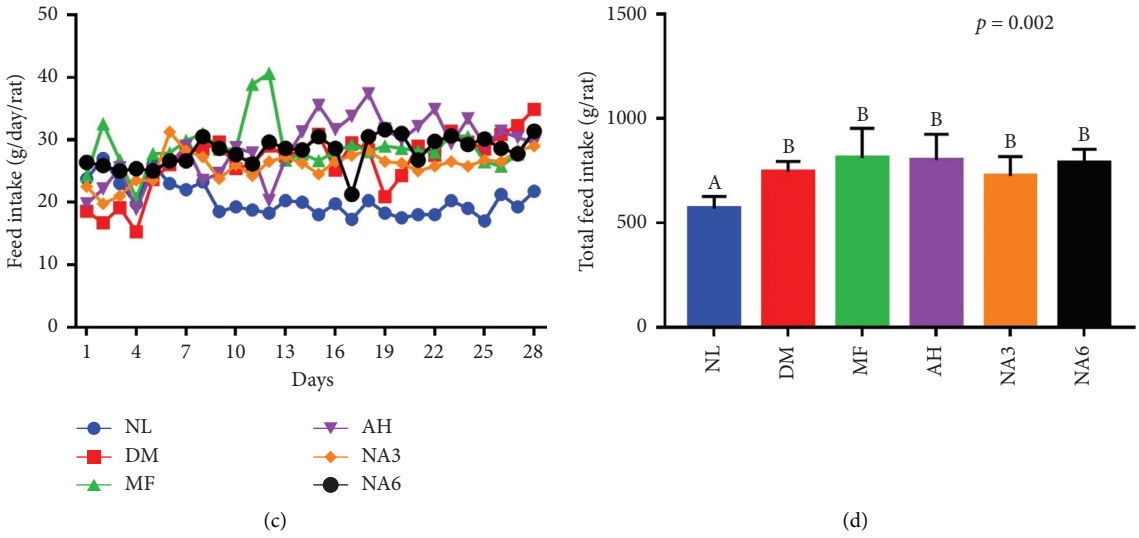



FIGURE 2: Effects of *Acalypha hispida* extract and nanoextract on water and feed consumption in diabetic rats. (a) The profile of water intake for 28 days, (b) total water intake for 28 days, (c) the profile of feed intake for 28 days, and (d) total feed intake for 28 days. Values are demonstrated as the mean ± SD ($n = 5$). Identical letters (A–B) mean no significant differences in DMRT ($\alpha = 0.05$).

*A. hispida* nanoextract at 60 mg/kg body weight increased insulin secretion in diabetic rats (Figure 3(g)). This ability is thought to be related to rutin and quercetin, which increase insulin secretion in diabetic rats [34]. Quercetin enhances mitochondrial bioenergetic function, resulting in increased ATP production and $Ca^{2+}$ ion levels, which initiate the priming of insulin vesicles for exocytosis [34]. Rutin participates in insulin secretagogue activity by amplifying pathways such as the PLC/PKC and cAMP/PKA signaling cascades, thereby enhancing glucose-induced insulin secretion [34].

Previous reports have shown that plant extracts can help in treating STZ/Alloxan-induced diabetic rats by increasing or maintaining pancreatic $\beta$-cell counts and insulin secretion. A study found that *Laurus nobilis* leaf extract improved the regeneration of pancreatic islets [35]. Another study discovered that administering ginger (*Zingiber officinale* var. Amarum) and pigeonpea (*Cajanus cajan*) leaf extracts for 28 days decreased blood glucose levels and improved body weight, insulin levels, and $\beta$-cell counts in diabetic rats [24]. In addition, research has shown that *Hibiscus rosa-sinensis* leaf extract increases insulin release by inducing depolarization and increasing intracellular $Ca^{2+}$ levels in BRIN-BD11 cells [36].

Figures 4(a) and 4(b) display photomicrographs of H3K9Ac staining in the islets of Langerhans and acinar cells. The intensity of the 3,3′-diaminobenzidine (DAB) signal is shown in Figures 4(c) and 4(d). The MET, AH, NA3, and NA6 groups demonstrated significantly lower total H3K9Ac levels than the DM group ($p = 0.045$). The extract and nanoextracts reduced total H3K9AC levels in the islets of Langerhans but not in the acinar cells in all groups ($p = 0.293$). The results showed that STZ-induced diabetic rats experienced alterations in histone H3 epigenetics only in the islets of Langerhans, not in the acinar cells. However, treatment with *A. hispida* nanoextract in diabetic rats abrogated histone H3K9Ac epigenetic alterations. This activity is associated with rutin, which efficiently abrogates histone acetyltransferase (HAT) activity [37]. HAT is responsible for transferring an acetyl group from acetyl-CoA to the $\varepsilon$-amino group of a lysine residue. Consequently, H3K9Ac levels in the islets of Langerhans decreased after *A. hispida* nanoextract treatment.

Histone modifications play a role in regulating insulin gene expression and pancreatic beta cells [38]. Previous studies have shown an increase in total H3K9Ac levels in the pancreas of diabetic rats [10]. However, this increase in total H3K9Ac was not associated with genes such as Pdx1 (involved in insulin expression and $\beta$-cell development), Pax4 (involved in $\beta$-cell development and function), Insulin, and Bcl2 (an inhibitor of apoptosis) in the pancreas of diabetic rats [10]. In addition, an increase in total H3K9Ac is associated with the upregulation of the Caspase-3 gene, which is linked to proapoptotic activity [10]. Therefore, the proposed mechanism of *A. hispida* treatment in diabetic rats involves the inhibition of HAT activity, resulting in decreased total H3K9Ac and the subsequent inactivation of Caspase-3.

The hepatic glycogen content of diabetic rats treated with *A. hispida* is shown in Figure 5(a). The MF, AH, and NA6 groups demonstrated significantly higher glycogen content than the DM group ($p < 0.001$; Figure 5(b)). Thus, the extract (300 mg/kg body weight) and nanoextract (60 mg/kg body weight) increased glycogen content in the livers of diabetic rats. The treatment of the extract and nanoextracts to diabetic rats elevated the hepatic glycogen levels (Figure 5). STZ-treated rats exhibit increased glycogenolysis [39]. This study also showed that diabetic rats showed increased glycogenolysis, as evidenced by a reduction in glycogen content in the liver (Figure 5). This increase in gluconeogenesis and decrease in glycogenolysis are partly due to elevated levels of insulin in the blood, which increases glycogenesis (glycogen

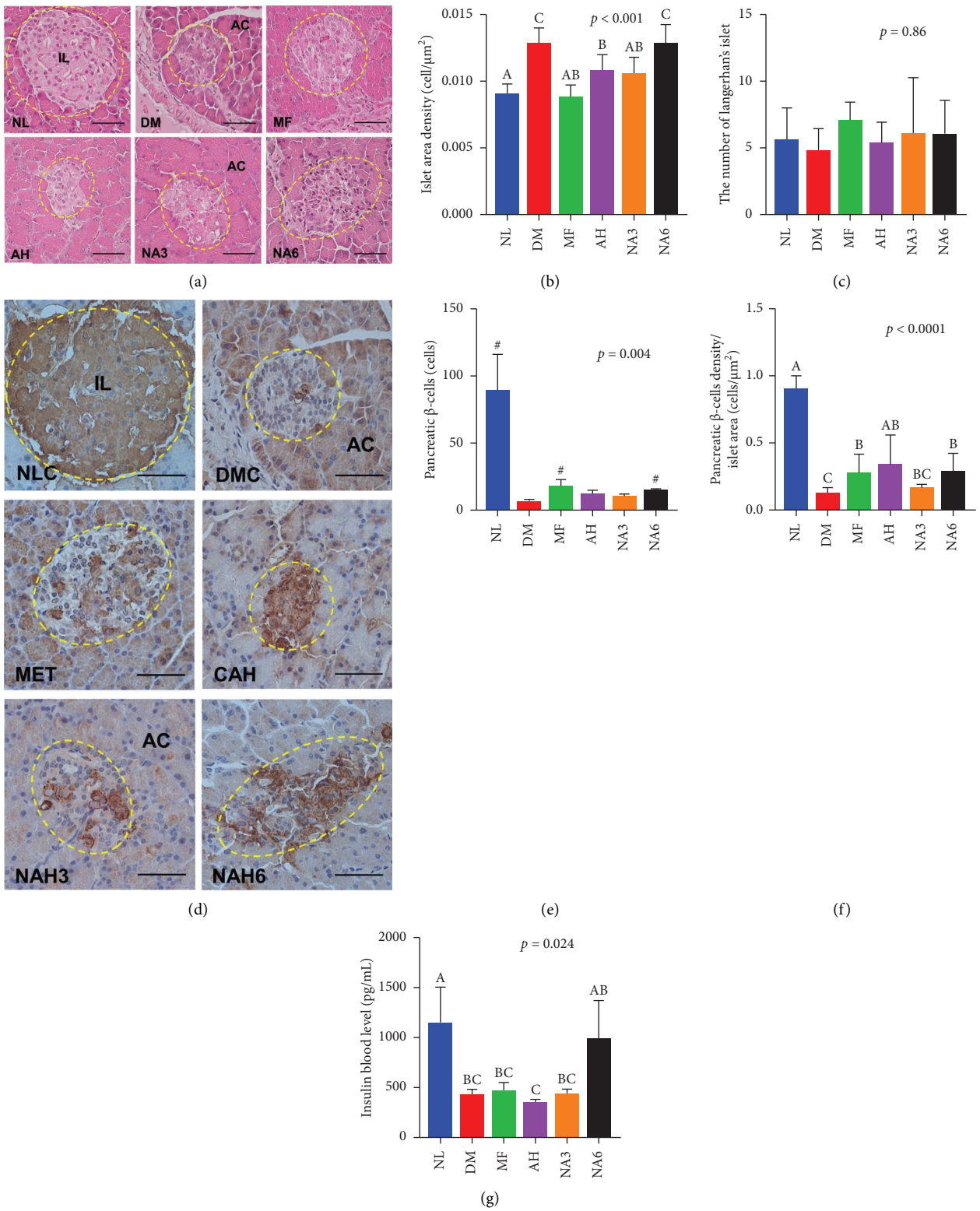



FIGURE 3: Effects of *Acalypha hispida* extract and nanoextract on pancreatic tissue and insulin levels. (a) Hematoxylin-eosin staining, (b) islet area density (cell/μm$^2$), (c) number of islets of Langerhans, (d) insulin staining, (e) pancreatic β-cell/islets of Langerhans ratio, (f) pancreatic β-cell density/islet area (cells/$\mu$m$^2$), and (g) insulin blood level (pg/mL). Values are presented as the mean ± SD ($n = 5$). Scale = 50 μm. Magnification = 400x. Identical letters (A–C) mean no significant differences in DMRT ($\alpha = 0.05$). The Mann–Whitney test demonstrations significant differences: NL (# < 0.01), MF (# < 0.01), and NA6 (# < 0.01) vs. DM group.

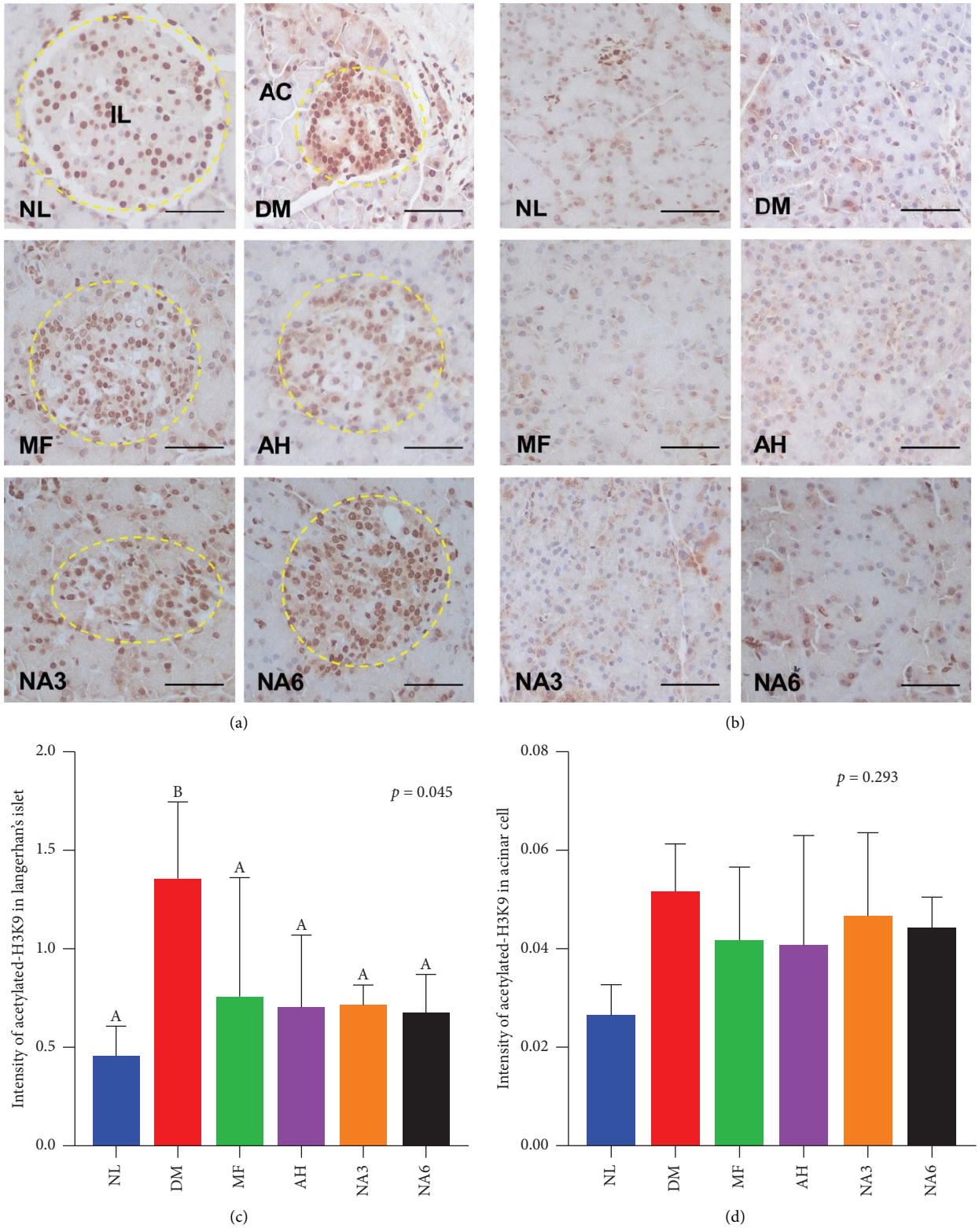
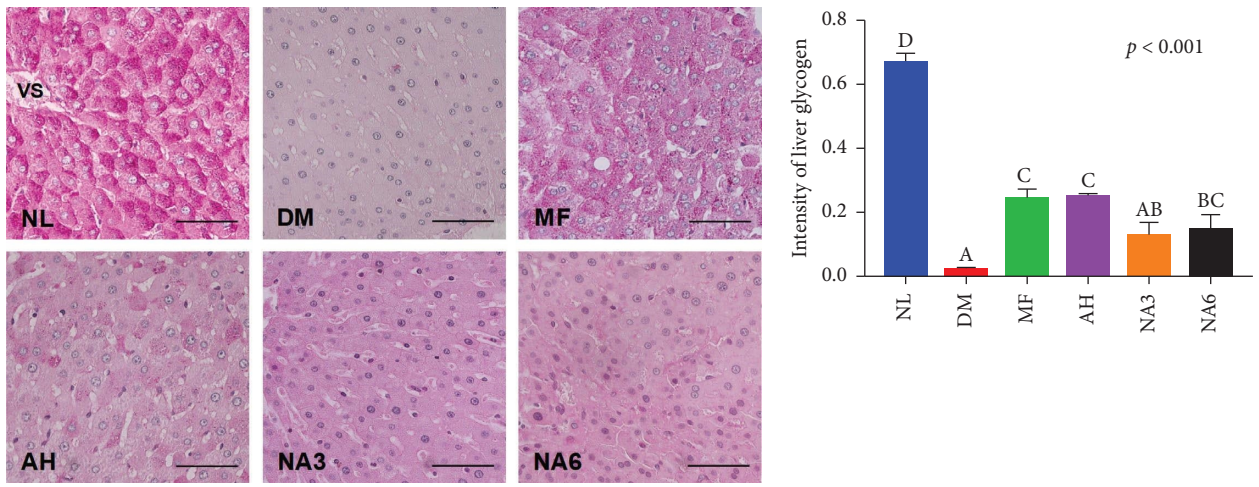



Figure 4: Effects of the *Acalypha hispida* extract and nanoextract on total acetylated histone H3 in the pancreas of diabetic rats. (a) Islets of Langerhans (PL); (b) acinar cells (SA); (c) intensity of the DAB signal of H3K9Ac-positive cells in islets of Langerhans; and (d) intensity of the DAB signal of H3K9Ac-positive cells in acinar cells. Values are presented as the mean ± SD ($n = 5$). Scale = 50 $\mu$m. Magnification = 400x. Identical letters (A–C) mean no significant differences in DMRT ($\alpha = 0.05$).




(a) (b)

Figure 5: Effects of *Acalypha hispida* extract and nanoextract on glycogen content in the livers of diabetic rats. (a) Periodic acid-Schiff staining of the liver. (b) Intensity of glycogen content in the liver. Values are presented as the mean ± SD ($n = 5$). Scale = 50 $\mu$m. Magnification = 400x. Identical letters (A–D) mean no significant differences in DMRT ($\alpha = 0.05$).

synthesis) and the uptake of glucose into cells, such that glycogen in the liver does not break down continuously [40]. A previous study reported that *Sapium ellipticum* leaf extract increased the glycogen content in the liver and muscle of diabetic rats and simultaneously increased insulin levels [39]. The water extract of *Potentilla discolor* enhances the liver glucose balance by controlling gluconeogenesis and glycogen synthesis in mice with type 2 diabetes induced by a high-fat diet and STZ [41].

Figure 6(a) shows a photomicrograph of H3K9Ac staining in the liver and Figure 6(b) shows its intensity. Significantly higher total H3K9Ac levels were observed in the DM group than those in in the NL, MF, NA3, and NA6 groups. This result revealed that the nanoextract reduced total H3K9Ac levels in the diabetic rat liver. This finding was also supported by a previous research, revealing that increased H3K9Ac levels in the liver cause the development of diabetes via the dysregulation of hepatic glucose production and lipogenesis [42]. This mechanism is supported by an increase in glucose production through glycogenolysis (Figures 1(b) and 5(b)) and increased lipolysis, as indicated by increased TC, TG, and VLDL levels in the serum (Figure 7).

Previous research has shown that acetylation is H3K9 in the livers of diabetic mice. Furthermore, the increase in H3K9Ac was associated with a decrease in the mRNA expression of glucose transporter-2 (GLUT2), glucokinase (Gck), pyruvate kinase (Pklr), and insulin receptor (Insr) [43]. Exendin-4 treatment reduced H3K9Ac levels in diabetic mice [43].

There was no significant change in hematological profiles among groups ($p > 0.05$; Figure 8). This result indicates that the extract and nanoextract did not change the hematological profile of rats.

The effect of *A. hispida* nanoextract on the lipid profile is shown in Figures 7(a), 7(b), 7(c), 7(d). The MF, AH, and NA6 groups had significantly lower TC levels than the DM group ($p = 0.007$). Moreover, the DM group exhibited significantly elevated levels of TG and VLDL compared with the NL, MF, and NA6 groups (Figures 7(b) and 7(d)). TG and VLDL levels were not significantly different among the MF, AH, and NA6 groups ($p = 0.028$). HDL levels were also not significantly different among the groups ($p = 0.70$; Figure 7(c)). The MF, AH, NA3, and NA6 groups showed a significantly lower AI compared with the DM group ($p = 0.001$; Figure 7(e)).

Lipid metabolism disorders in STZ-induced diabetic rat models are caused by insulin deficiency, which stimulates lipid breakdown (lipolysis) in the bloodstream. In fat cells (adipocytes), triglycerides are broken down into fatty acids and glycerols via lipolysis [44]. TC, TG, and VLDL levels show a significant increase in diabetic rats [45]. In this study, the extract and nanoextract (60 mg/kg body weight) exhibited hypolipidemic effects in diabetic rats, as shown by a decrease in TC, TG, and VLDL levels and reduced risk of atherosclerosis. The ability of *A. hispida* nanoextract in the NA6 group to reduce TC and TG levels was related to increased insulin levels (Figure 3(g)). Insulin inhibits lipolysis by inhibiting adipose triglyceride lipase (ATGL) via Egr1-mTORC1, FoxO1-SIRT1, and SP1 signaling [7]. Insulin also suppresses HSL [46]. In a previous study, diabetic rats exhibited increased levels of TC, TG, and LDL and decreased levels of HDL. Treatment with the olive leaf extract for 70 days resulted in a reduction in TC, TG, and LDL levels and an increase in HDL levels [47].

PCA showed that the groups were separated into three clusters in PC1 with a variation of 35.7% (Figure 9(a)). The DM group was negative for PC1, whereas the NL group was positive for PC1. These results illustrate that PC1 separated diabetic and normal conditions. Diabetic rats treated with the extract, nanoextract, or metformin were between these conditions. Thus, the administration of extract, nanoextract, and metformin improved diabetic conditions. The

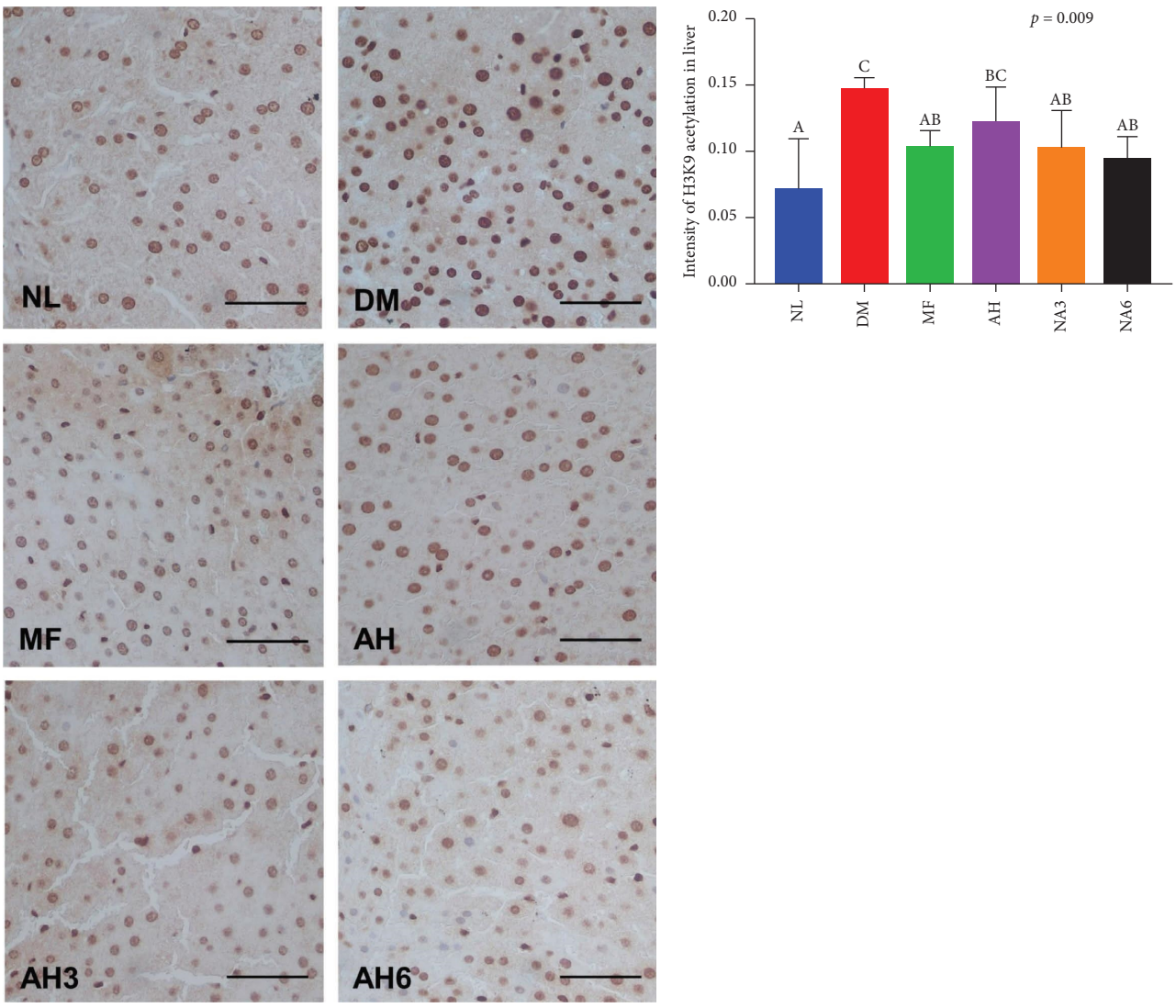



Figure 6: Effects of *Acalypha hispida* extract and nanoextract on total acetylated histone H3 in the liver of diabetic rats. (a) Immunohistochemistry for H3Ac in the liver. (b) Intensity of the DAB signal in H3K9Ac-positive cells in the liver. Values are presented as the mean ± SD ($n = 5$). Scale = 50 μm. Magnification = 400x. Identical letters (A–C) mean no significant differences in DMRT ($\alpha = 0.05$).

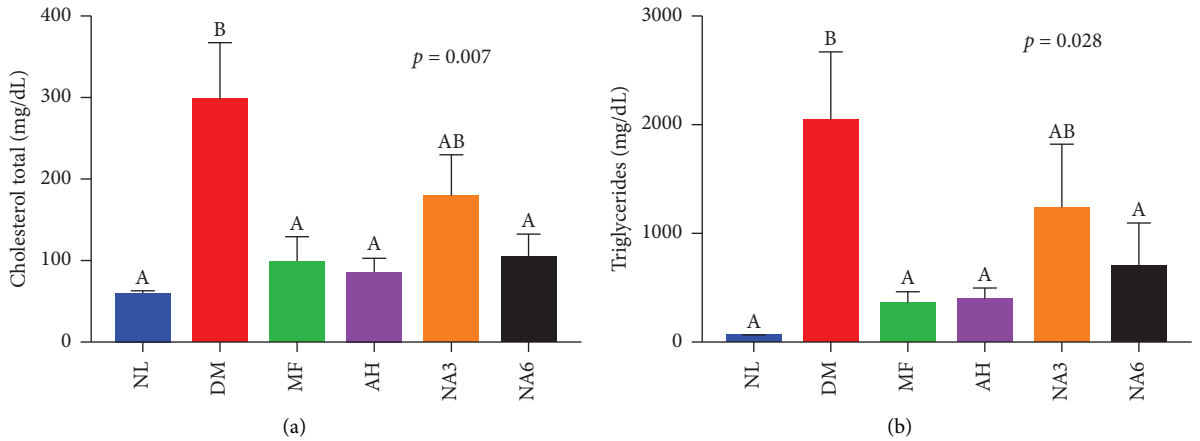



Figure 7: Continued.

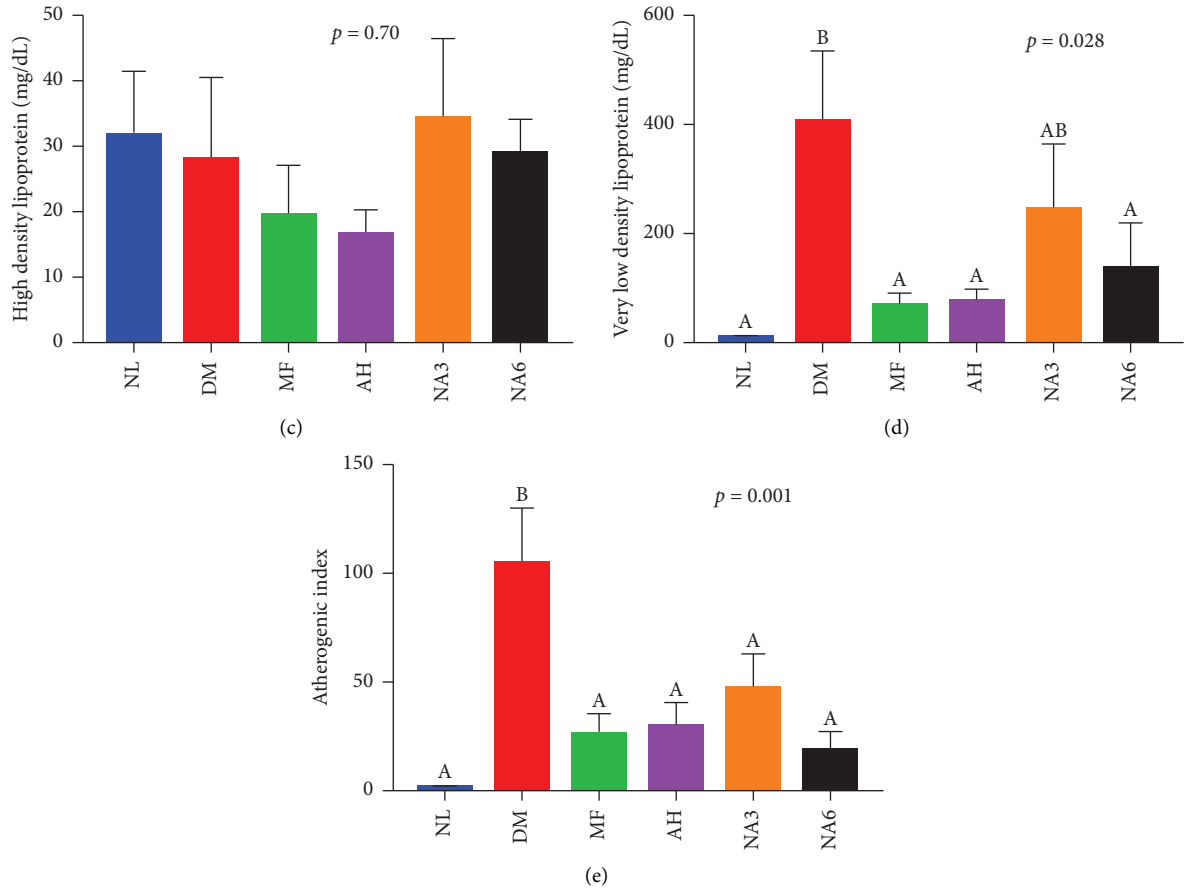



Figure 7: Effects of *Acalypha hispida* extract and nanoextract on lipid profiles of diabetic rats. (a) Total cholesterol, (b) triglycerides, (c) high-density lipoprotein (HDL), (d) very low-density lipoprotein (VLDL), and (e) atherogenic index. Values are presented as the mean ± SD ($n = 5$). Identical letters (A–C) mean no significant differences in DMRT ($\alpha = 0.05$).

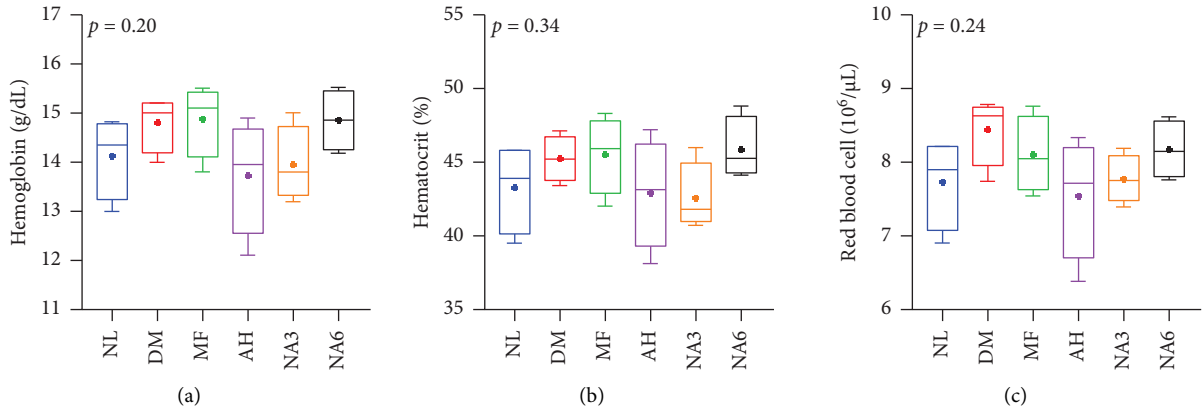



Figure 8: Continued.

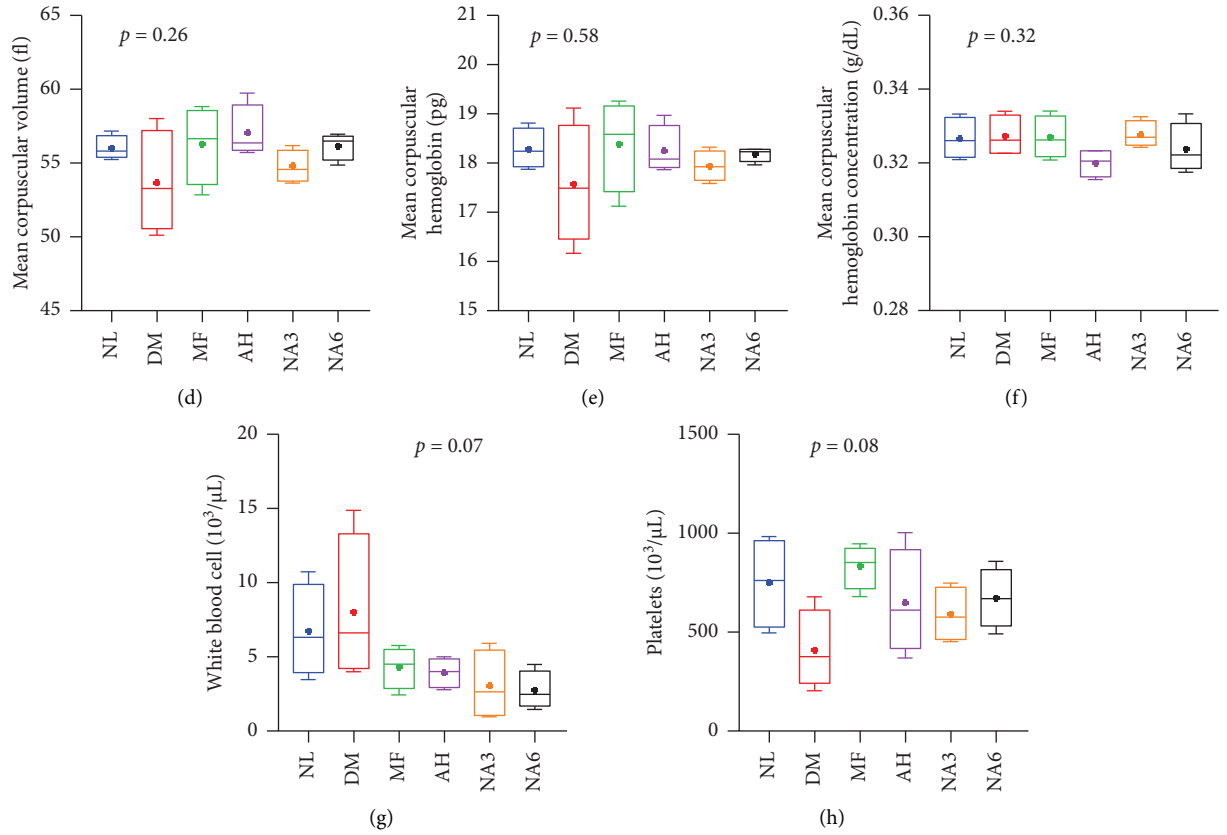



Figure 8: Effects of *Acalypha hispida* extract and nanoextract on the hematological profile of diabetic rats. (a) Hemoglobin, (b) hematocrit, (c) red blood cells, (d) mean corpuscular volume, (e) mean corpuscular hemoglobin, (f) mean corpuscular hemoglobin concentration, (g) white blood cells, and (h) platelets. Values are presented as the mean ± SD ($n = 5$).

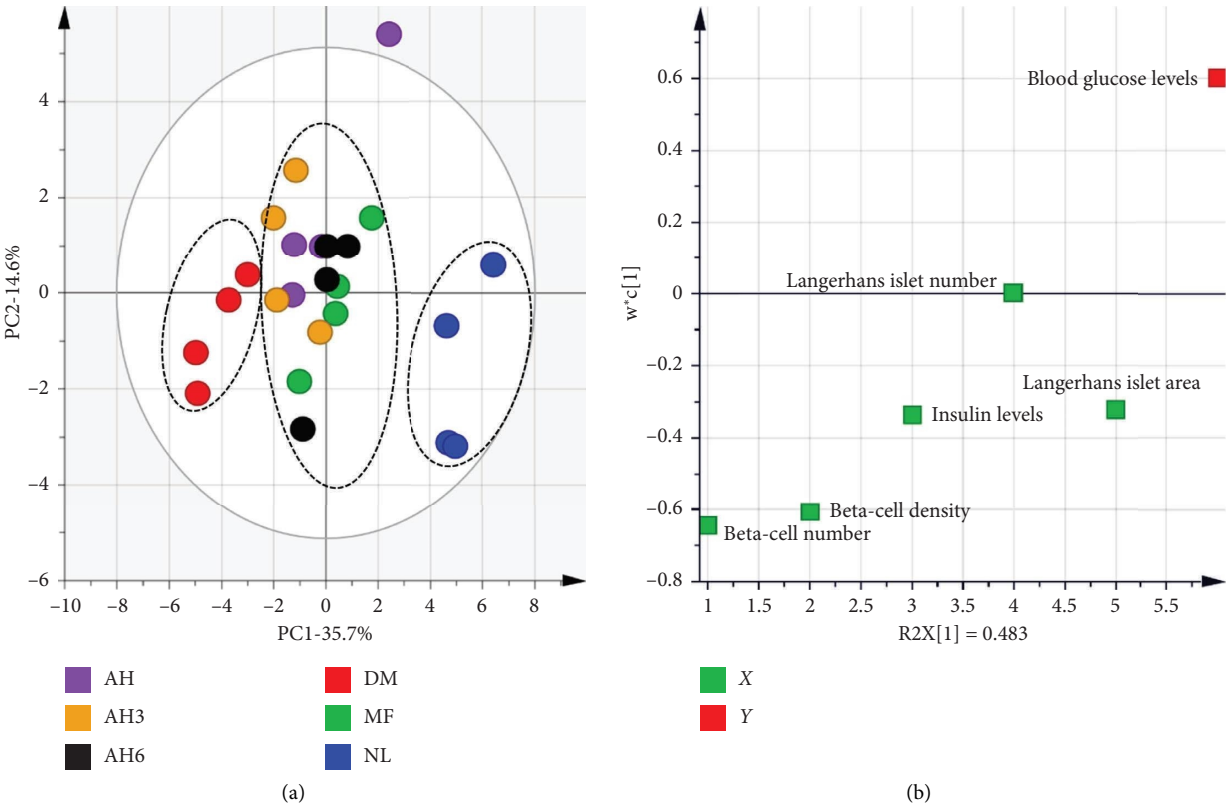



Figure 9: Multivariate analysis of all parameters. (a) Scatter plot of principal component analysis (PCA). (b) Loading plot of partial least squares (PLS) of parameters related to decreased blood glucose levels.

Table 4: Value of the variable influence on the projection (VIP) of the parameters is directly related to decreased blood glucose levels.

| Var ID (primary) | M1.VIP[1] | 2.44693*M1.VIP[1]cvSE |
|---|---|---|
| Beta-cell number | 1.43964 | 0.333478 |
| Beta-cell density | 1.35947 | 0.477993 |
| Insulin level | 0.746326 | 0.924301 |
| Islet of Langerhan's area | 0.722679 | 0.750144 |
| Islet of Langerhan's number | 0.00144423 | 0.329076 |

*Note:* M1.VIP[1]: Variable importance in the projection (VIP). 2.44693*M1.VIP[1]cvSE: VIP score multiplied by a constant (2.44693) and the cross-validated standard error (cvSE) used in assessing the significance or reliability of the variable's contribution to the model. $R^2Y = 0.854$, and $Q^2 = 0.821$.

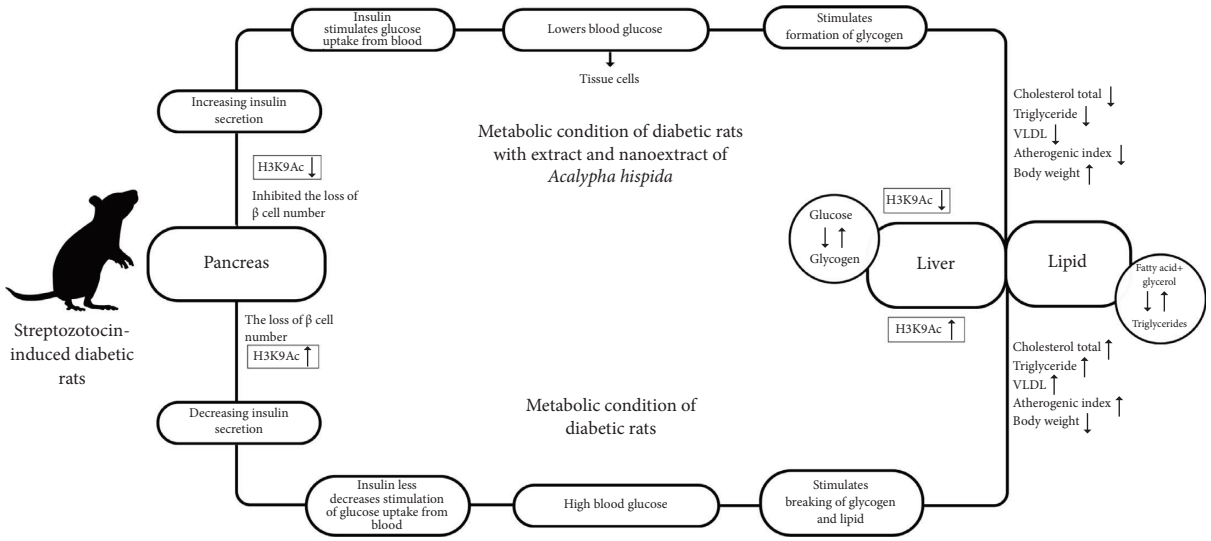



Figure 10: Antidiabetic mechanisms of extract and nanoextract of *Acalypha hispida*. Extract and nanoextract inhibited the loss of $\beta$-cell number and increased insulin secretion in the bloodstream. Insulin secretion is associated with decreased lysine 9 acetylation of histone 3 (H3K9Ac) in islets of langerhans. Insulin stimulates glucose uptake from the blood into tissue cells, thereby decreasing blood glucose levels. In addition, increased insulin levels promote glycogen and triglyceride formation. Glycogen formation is associated with decreased H3K9Ac levels in the liver. Consequently, total cholesterol, triglyceride, and very low-density lipoprotein (VLDL) levels and the atherogenic index decreased in the blood, and body weight increased.

nanoextract at a dose of 60 mg/kg body weight tended to approach normal conditions compared with the crude extract and nanoextract at a dose of 30 mg/kg.

The nanoextract at a dose of 60 mg/kg body weight exhibited a better effect than the extract at a dose of 300 mg/kg body weight, even though the dose was 5-fold smaller. This increased pharmacological effect was influenced by the nanosizing of the extract. Nanoscale particles enhance bioavailability and bioactivity [17]. Therefore, the nanosizing of the extract in the present study was useful for reducing the administered dose. Although the levels of the bioactive compounds decreased after milling, the antidiabetic effects of the extract increased. The milling process generates nanoscale materials via the impact force generated by the centrifugal force [48]. In the field of biomedicine, nanoparticles affect drug stability, release profiles, biodistribution, mucoadhesion, and uptake [19].

Partial least squares (PLS) showed an $R^2Y$ value of 0.854 and a $Q^2$ value of 0.821 (Figure 9(b)). $R^2Y$ and $Q^2$ values $\geq 0.5$ indicate a stable and reliable model [49]. Based on the score of variable importance on projection (VIP), the parameters that most influenced blood glucose levels were pancreatic $\beta$-cell number and density as indicated by VIP score > 1 (Table 4). If the VIP value is greater than 1, the variable is considered "important," whereas a value below 0.5 indicates the variable is "unimportant." The range between 0.5 and 1 is ambiguous, as the importance level varies based on the size of the dataset [50]. VIP scores indicate the importance of each variable in elucidating the variance in the dependent variables ($Y$ variables) governed by the PLS components.

According to the findings of this study, the antidiabetic mechanisms of the extract and nanoextract of *A. hispida* are shown in Figure 10. Extract and nanoextract exhibited significant inhibition of $\beta$-cell loss, indicating their potential to preserve pancreatic islet functionality. These effects were indicated by PLS, which showed that $\beta$-cell number and density were important in decreasing blood glucose levels (Figure 9(b), Table 4). The nanoextracts also stimulated insulin secretion, resulting in decreased blood glucose levels. The mechanism underlying this effect was associated with decreased H3K9Ac levels, which facilitated the transcriptional

activity of insulin-related genes. Consequently, elevated insulin levels promoted glucose uptake from the bloodstream into cells. The promotion of glycogen formation was linked to a reduction in H3K9Ac levels, highlighting its role in improving glucose homeostasis. In addition, enhanced insulin signaling led to the formation of glycogen and triglycerides, contributing to decreases in total cholesterol, triglyceride, VLDL levels, and AI in the blood. The administration of the extract and nanoextract resulted in increased body weight, indicating improved overall metabolic health. These effects were supported by PCA, which showed that diabetic rats administrated with both extract and nanoextract formed a cluster separate from that of untreated diabetic rats (Figure 9(a)).

However, the present findings have potential limitations, particularly regarding the preparation of herbal nanoparticles. The nanoextract of *A. hispida* remained at approximately 733 nm, which affected its bioavailability and efficacy for the treatment of diabetes. In future studies, the nanomilling process could be optimized to produce nanoextract powder under 100 nm, which would increase bioavailability and reduce the required dose.

## 4. Conclusions

The extract and nanoextract of *A. hispida* leaf exhibited antidiabetic effects as indicated by the following parameters: decreased blood glucose levels, increased pancreatic β-cell number and density, increased insulin levels, decreased H3K9Ac levels in the islets of Langerhans and liver, enhanced hepatic glycogen levels, and improved lipid metabolism (TC, TG, VLDL, and AI). Moreover, PCA indicated that the nanoextract (60 mg/kg body weight) demonstrated the best antidiabetic effect in terms of these parameters. β-cell number and density were identified as parameters that contributed to the decrease in blood glucose levels. Overall, *A. hispida* extract and nanoextract exert antidiabetic effects by restoring β-cell number and density via decreasing H3K9Ac levels in the islets of Langerhans in STZ-induced diabetic rats.

## Data Availability Statement

The data that support the findings of this study are available from the corresponding author on request.

## Conflicts of Interest

The authors declare no conflicts of interest.

## Funding

This work was supported by a Post-Doctoral 2023 grant from the IPB University (number: 9/IT3/SP/WCU/2023).

## Acknowledgments

This work was supported by a Postdoctoral 2023 grant from the IPB University (number: 9/IT3/SP/WCU/2023). We would like to thank Editage (https://www.editage.com) for editing and reviewing this manuscript for English language.

## References

[1] International Diabetes Federation, *International Diabetes Federation* (Brussels, Belgium: IDF, 2021).

[2] A. Sameer, M. Banday, and S. Nissar, "Pathophysiology of Diabetes: An Overview," *Avicenna Journal of Medicine* 10, no. 4 (2020): 174–188, https://doi.org/10.4103/ajm.ajm_53_20.

[3] R. Ajjan, D. Slattery, and E. Wright, "Continuous Glucose Monitoring: A Brief Review for Primary Care Practitioners," *Advances in Therapy* 36, no. 3 (2019): 579–596, https://doi.org/10.1007/s12325-019-0870-x.

[4] American Diabetes Association Ada, "Standards Of Medical Care in Diabetes-2022 Abridged for Primary Care Providers," *Clinical Diabetes* 40, no. 1 (2022): 10–38, https://doi.org/10.2337/cd22-as01.

[5] F. J. Pasquel, M. C. Lansang, K. Dhatariya, and G. E. Umpierrez, "Management of Diabetes and Hyperglycaemia in the Hospital," *Lancet Diabetes & Endocrinology* 9, no. 3 (2021): 174–188, https://doi.org/10.1016/S2213-8587(20)30381-8.

[6] A. Chaudhury, C. Duvoor, V. S. Reddy Dendi, et al., "Clinical Review of Antidiabetic Drugs: Implications for Type 2 Diabetes Mellitus Management," *Frontiers in Endocrinology* 8, no. January (2017): 6, https://doi.org/10.3389/fendo.2017.00006.

[7] D. Li, L. Zhang, Y. He, et al., "Novel Histone Post-Translational Modifications in Diabetes and Complications of Diabetes: The Underlying Mechanisms and Implications," *Biomedicine & Pharmacotherapy* 156, no. November (2022): 113984, https://doi.org/10.1016/j.biopha.2022.113984.

[8] A. Gansen, K. Tóth, N. Schwarz, and J. Langowski, "Opposing Roles of H3- and H4-Acetylation in the Regulation of Nucleosome Structure-A FRET Study," *Nucleic Acids Research* 43, no. 3 (2015): 1433–1443, https://doi.org/10.1093/nar/gku1354.

[9] S. Kaimala, C. A. Kumar, M. Z. Allouh, S. A. Ansari, and B. S. Emerald, "Epigenetic Modifications in Pancreas Development, Diabetes, and Therapeutics," *Medicinal Research Reviews* 42, no. 3 (2022): 1343–1371, https://doi.org/10.1002/med.21878.

[10] P. Tu, B. Huang, M. Li, et al., "Exendin-4 May Improve Type 2 Diabetes by Modulating the Epigenetic Modifications of Pancreatic Histone H3 in STZ-Induced Diabetic C57BL/6 J Mice," *Journal of Physiology & Biochemistry* 78, no. 1 (2021): 51–59, https://doi.org/10.1007/s13105-021-00835-8.

[11] M. Tangkiatkumjai, H. Boardman, and D. M. Walker, "Potential Factors that Influence Usage of Complementary and Alternative Medicine Worldwide: A Systematic Review," *BMC Complementary Medicine and Therapies* 20, no. 1 (2020): 363–415, https://doi.org/10.1186/s12906-020-03157-2.

[12] J. M. Cardiel, A. A. C. de Sousa, I. Cordeiro, et al., "Updated Synopsis of Acalypha (Euphorbiaceae, Acalyphoideae) from Brazil," *Plant Systematics and Evolution* 308, no. 4 (2022): 24–38, https://doi.org/10.1007/s00606-022-01816-0.

[13] J. I. Achika, A. J. Yusuf, R. G. Ayo, and D. U. Liman, "Flavonoids From Nigerian Indigenous Medicinal Plants and Their Bioactivities: A Review," *Phytomedicine* 3, no. 2 (2023): 100405, https://doi.org/10.1016/j.phyplu.2023.100405.

[14] P. Prajna, R. Reshmi, K. Shana, V. Vishnupriya, P. Fahmeeda, and E. Jothi, "Traditional Uses,

Phytochemistry and Pharmacology of Acalypha Hispida Burm: A Systematic Review," *World Journal of Biology Pharmacy and Health Sciences* 12, no. 2 (2022): 087–093, https://doi.org/10.30574/wjbphs.2022.12.2.0194.

[15] H. Alfarisi, S. S. Diah, and T. Wresdiyati, "Polyphenol Profile, Antioxidant and Hypoglycemic Activity of Acalypha Hispida Leaf Extract," *Indian Journal of Pharmaceutical Sciences* 82, no. 2 (2020): 291–299, https://doi.org/10.36468/pharmaceutical-sciences.649.

[16] H. Alfarisi, M. Subangkit, S. Sa'diah, and T. Wresdiyati, "Acute Toxicity Test of Ethanolic Extract of Acalypha Hispida Leaves in Female Rats: A Physiological and Histological Study," *Jurnal Kedokteran Hewan-Indonesian Journal of Veterinary Sciences* 14, no. 3 (2020): 48–53, https://doi.org/10.21157/j.ked.hewan.v14i3.16176.

[17] T. Gunasekaran, T. Haile, T. Nigusse, and M. D. Dhanaraju, "Nanotechnology: An Effective Tool for Enhancing Bioavailability and Bioactivity of Phytomedicine," *Asian Pacific Journal of Tropical Biomedicine* 4, no. Suppl 1 (2014): S1–S7, https://doi.org/10.12980/APJTB.4.2014C980.

[18] G. Ratheesh, Y. Xiao, H. Ezhilarasu, et al., "Nanodrug Delivery System Using Medicinal Plants," in *Drug Delivery Nanosystems for Biomedical Applications*, ed. C. P. Sharma (Oxford, UK: Elsevier, 2018), 357–375.

[19] A. El-Sayed and M. Kamel, "Advanced Applications of Nanotechnology in Veterinary Medicine," *Environmental Science & Pollution Research* 27, no. 16 (2020): 19073–19086, https://doi.org/10.1007/s11356-018-3913-y.

[20] H. Alfarisi, S. Sa'diah, B. Juliandi, and T. Wresdiyati, "Preparation and Characterization of Nanopowder of Acalypha Hispida Leaves Extract Using Planetary Ball Milling," *Molekul* 17, no. 1 (2022): 68, https://doi.org/10.20884/1.jm.2022.17.1.5601.

[21] H. Alfarisi, T. Wresdiyati, S. Sadiah, and B. Juliandi, "Nanoextract of Acalypha Hispida Leaves Increases Antioxidant Defense and Suppresses Microstructure Damage in Liver and Kidney of Diabetic Rats," *Journal of Applied Pharmaceutical Science* 12, no. 10 (2022): 99–108, https://doi.org/10.7324/JAPS.2022.121010.

[22] T. Wresdiyati, S. Sa'diah, M. Astawan, et al., "The Repeated Dose 28-Day Oral Toxicity Study of Combined Extract of Cajanus Cajan Leaf and *Zingiber officinale* Rhizome in Male and Female Sprague-Dawley Rats," *Tropical Journal of Natural Product Research* 7, no. 8 (2023): 3706–3716, https://doi.org/10.26538/tjnpr/v7i8.21.

[23] J. A. Kiernan, *Histological and Histochemical Methods* (Banbury, UK: Scion Publishing Ltd, 2015).

[24] T. Wresdiyati, S. Sa'diah, S. A. Azis, M. Darawati, and H. Alfarisi, "Assessment of Anti-Diabetic Activity of Cajanus Cajan Leaf and *Zingiber officinale* Extracts in the Alloxan-Diabetic Rats," *IOP Conference Series: Earth and Environmental Science* 2024, no. 1359 (2024): 012128, https://doi.org/10.1088/1755-1315/1359/1/012128.

[25] S. H. Park, Y. E. Sim, M. K. Kang, et al., "Purple Perilla Frutescens Extracts Containing $\alpha$-asarone Inhibit Inflammatory Atheroma Formation and Promote Hepatic HDL Cholesterol Uptake in Dyslipidemic apoE-Deficient Mice," *Nutrition Research and Practice* 17, no. 6 (2023): 1099–1112, https://doi.org/10.4162/nrp.2023.17.6.1099.

[26] A. Crowe and W. Yue, "Semi-Quantitative Determination of Protein Expression Using Immunohistochemistry Staining and Analysis: An Integrated Protocol," *Bio-Protocol* 9, no. 24 (2019): 34655–e3511, https://doi.org/10.21769/BioProtoc.3465.

[27] S. Zaqout, L. L. Becker, and A. M. Kaindl, "Immunofluorescence Staining of Paraffin Sections Step by Step," *Frontiers in Neuroanatomy* 14, no. November (2020): 582218–582311, https://doi.org/10.3389/fnana.2020.582218.

[28] T. Wresdiyati, S. Sa'diah, and A. Winarto, "The Antidiabetic Properties of Indonesian Swietenia Mahagoni in Alloxan Induced-Diabetic-Rats," *World Academy of Science, Engineering and Technology* 10, no. 10 (2016): 631–637, https://doi.org/10.5281/zenodo.1126884.

[29] S. Karthik, R. Suriyaprabha, K. S. Balu, P. Manivasakan, and V. Rajendran, "Influence of Ball Milling on the Particle Size and Antimicrobial Properties of Tridax Procumbens Leaf Nanoparticles," *IET Nanobiotechnology* 11, no. 1 (2017): 12–17, https://doi.org/10.1049/iet-nbt.2016.0028.

[30] G. Rena, D. G. Hardie, and E. R. Pearson, "The Mechanisms of Action of Metformin," *Diabetologia* 60, no. 9 (2017): 1577–1585, https://doi.org/10.1007/s00125-017-4342-z.

[31] I. Fajarwati, D. D. Solihin, T. Wresdiyati, and I. Batubara, "Self-Recovery in Diabetic Sprague Dawley Rats Induced by Intraperitoneal Alloxan and Streptozotocin," *Heliyon* 9, no. 5 (2023): e15533, https://doi.org/10.1016/j.heliyon.2023.e15533.

[32] F. Haghani, M. R. Arabnezhad, S. Mohammadi, and A. Ghaffarian-Bahraman, "Aloe Vera and Streptozotocin-Induced Diabetes Mellitus," *Revista Brasileira de Farmacognosia* 32, no. 2 (2022): 174–187, https://doi.org/10.1007/s43450-022-00231-3.

[33] H. Alfarisi, S. Sa'diah, T. Wresdiyati, and B. Juliandi, "Nano-Extract of Acalypha Hispida Increased Cu,Zn-SOD Antioxidant in Pancreas of Diabetic Rat," *Indonesian Journal of Pharmaceutical Science and Technology* 10, no. 2 (2023): 82, https://doi.org/10.24198/ijpst.v10i2.37981.

[34] A. Ghorbani, R. Rashidi, and R. Shafiee-Nick, "Flavonoids for Preserving Pancreatic Beta Cell Survival and Function: A Mechanistic Review," *Biomedicine & Pharmacotherapy* 111 (2019): 947–957, https://doi.org/10.1016/j.biopha.2018.12.127.

[35] R. R. Mohammed, A. K. Omer, Z. Yener, A. Uyar, and A. K. Ahmed, "Biomedical Effects of *Laurus nobilis* L. Leaf Extract on Vital Organs in Streptozotocin-Induced Diabetic Rats: Experimental Research," *Annals of Medicine and Surgery* 61 (2021): 188–197, https://doi.org/10.1016/j.amsu.2020.11.051.

[36] P. Ansari, S. Azam, J. M. A. Hannan, P. R. Flatt, and Y. H. A. Abdel Wahab, "Anti-Hyperglycaemic Activity of H. Rosa-Sinensis Leaves Is Partly Mediated by Inhibition of Carbohydrate Digestion and Absorption, and Enhancement of Insulin Secretion," *Journal of Ethnopharmacology* 253, no. 2020 (2020): 112647, https://doi.org/10.1016/j.jep.2020.112647.

[37] J. Lee, J. H. Song, M. Y. Chung, et al., "3,4-Dihydroxytoluene, a Metabolite of Rutin, Suppresses the Progression of Non-alcoholic Fatty Liver Disease in Mice by Inhibiting P300 Histone Acetyltransferase Activity," *Acta Pharmacologica Sinica* 42, no. 9 (2021): 1449–1460, https://doi.org/10.1038/s41401-020-00571-7.

[38] W. Wang, Q. Shi, T. Guo, et al., "PDX1 and ISL1 Differentially Coordinate with Epigenetic Modifications to Regulate Insulin Gene Expression in Varied Glucose Concentrations," *Molecular and Cellular Endocrinology* 428 (2016): 38–48, https://doi.org/10.1016/j.mce.2016.03.019.

[39] O. M. Ighodaro and O. A. Akinloye, "Anti-Diabetic Potential of *Sapium ellipticum* (Hochst) Pax Leaf Extract in Streptozotocin (STZ)-Induced Diabetic Wistar Rats," *BMC Complementary and Alternative Medicine* 17, no. 1 (2017): 525, https://doi.org/10.1186/s12906-017-2013-8.

[40] S. Hædersdal, A. Lund, F. K. Knop, and T. Vilsbøll, "The Role of Glucagon in the Pathophysiology and Treatment of Type 2 Diabetes," *Mayo Clinic Proceedings* 93, no. 2 (2018): 217–239, https://doi.org/10.1016/j.mayocp.2017.12.003.

[41] T. Li, R. Chang, H. Zhang, M. Du, and X. Mao, "Water Extract of Potentilla Discolor Bunge Improves Hepatic Glucose Homeostasis by Regulating Gluconeogenesis and Glycogen Synthesis in High-Fat Diet and Streptozotocin-Induced Type 2 Diabetic Mice," *Frontiers in Nutrition* 7, no. September (2020): 161–212, https://doi.org/10.3389/fnut.2020.00161.

[42] J. Viscarra and H. S. Sul, "Epigenetic Regulation of Hepatic Lipogenesis: Role in Hepatosteatosis and Diabetes," *Diabetes* 69, no. 4 (2020): 525–531, https://doi.org/10.2337/dbi18-0032.

[43] P. Tu, X. Li, B. Ma, et al., "Liver Histone H3 Methylation and Acetylation May Associate with Type 2 Diabetes Development," *Journal of Physiology & Biochemistry* 71, no. 1 (2015): 89–98, https://doi.org/10.1007/s13105-015-0385-0.

[44] L. K. Townsend, C. M. Knuth, and D. C. Wright, "Cycling Our Way to Fit Fat," *Physics Reports* 5, no. 7 (2017): e13247–e13249, https://doi.org/10.14814/phy2.13247.

[45] A. I Airaodion, "Antidiabetic Effect of Ethanolic Extract of Carica Papaya Leaves in Alloxan-Induced Diabetic Rats," *American Journal of Biomedical Science & Research* 5, no. 3 (2019): 227–234, https://doi.org/10.34297/AJBSR.2019.05.000917.

[46] Y. L. Lan, J. C. Lou, W. Lyu, and B. Zhang, "Update on the Synergistic Effect of HSL and Insulin in the Treatment of Metabolic Disorders," *Therapeutic Advances in Endocrinology and Metabolism* 10 (2019): 2042018819877300–2042018819877310, https://doi.org/10.1177/2042018819877300.

[47] A. E.-M. M. R. Afify, H. S. El-Beltagi, S. A. Fayed, and A. E. El-Ansary, "Enhancing Effect of Olive Leaves Extract on Lipid Profile and Enzymes Activity in Streptozotocin Induced Diabetic Rats," *Fresenius Environmental Bulletin* 27, no. 3 (2018): 1875–1883.

[48] S. Bayda, M. Adeel, T. Tuccinardi, M. Cordani, and F. Rizzolio, "The History of Nanoscience and Nanotechnology: From Chemical–Physical Applications to Nanomedicine," *Molecules* 25, no. 1 (2019): 112, https://doi.org/10.3390/molecules25010112.

[49] L. Liang, G. Liu, G. Yu, F. Zhang, R. J. Linhardt, and Q. Li, "Urinary Metabolomics Analysis Reveals the Anti-Diabetic Effect of Stachyose in High-Fat Diet/Streptozotocin-Induced Type 2 Diabetic Rats," *Carbohydrate Polymers* 229, no. April 2019 (2020): 115534, https://doi.org/10.1016/j.carbpol.2019.115534.

[50] X. Tang and X. Zhang, "Dynamic Real Estate Project Cost Prediction Based on SIMCA-P," *IOP Conference Series: Earth and Environmental Science* 526, no. 1 (2020): 012178, https://doi.org/10.1088/1755-1315/526/1/012178.